

Reflection of two-gap nature in penetration depth measurements of MgB_2 film

Mun-Seog Kim, John A. Skinta, and Thomas R. Lemberger
Department of Physics, Ohio State University, Columbus, OH 43210-1106

W. N. Kang, Hyeong-Jin Kim, Eun-Mi Choi, and Sung-Ik Lee
National Creative Research Initiative Center for Superconductivity and Department of Physics, Pohang University of Science and Technology, Pohang 790-784, Republic of Korea
 (November 14, 2018)

The magnetic penetration depth, $\lambda(T)$, in the basal plane of a magnesium diboride (MgB_2) film was measured using a two-coil mutual inductance technique at 50 kHz. This film has $T_c \simeq 38$ K, $\Delta T_c \leq 1$ K, and $\lambda(0) \sim 1500$ Å. At low temperatures, $\lambda^{-2}(T)$ shows a clear exponential temperature dependence, indicating s -wave superconducting order parameter symmetry. However, the data are not quantitatively well described by theory assuming a single gap. From the data fit by the full BCS calculation assuming a double gap, the values of the two distinct gaps were obtained: $\Delta_S(0) = 2.61 \pm 0.41$ meV and $\Delta_L(0) = 6.50 \pm 0.33$ meV. The contributions of the small and the large gaps to the total superfluid density at $T = 0$ were estimated to be 21% and 79%, respectively. Finally, we consider the effect of gap anisotropy on the penetration depth measurements, and find that the gap anisotropy does not play a significant role in determining the temperature dependence of the penetration depth.

I. INTRODUCTION

Since the discovery of superconductivity in metallic MgB_2 , [1] abundant research has been carried out to elucidate its basic mechanism. MgB_2 has some notable features which contrast with cuprate superconductors. First, electron coupling is mediated by phonons, as indicated by the observation of a prominent isotope effect. [2] However, the transition temperature, $T_c \simeq 39$ K, might be somewhat higher than the theoretical prediction assuming a conventional phonon mechanism. [3] Recently, it was suggested that anisotropy in electron-phonon couplings plays a significant role in the unusually high transition temperature. [4,5] Secondly, many theoretical [4–7] and experimental works [8–20] suggest that MgB_2 has two separate gaps and that the symmetry of each gap is s -wave with a substantial gap anisotropy. The Fermi surface of MgB_2 consists of two nearly cylindrical (2D) sheets and two tubular networks (3D). [21] While the value of the gap associated with 3D sheets is in the range $0.5 \leq \Delta(0)/k_B T_c \leq 0.95$, for 2D networks the value is about $1.8 \leq \Delta(0)/k_B T_c \leq 2.2$. This double-gap structure and its anisotropic nature would be expected to play an important role in the physical properties of the compound.

In the early stages of MgB_2 study, a number of groups claimed unconventional superconductivity [22] or s -wave order parameter symmetry [23–25] from penetration depth measurements on various forms of samples. For example, Prozorov *et al.* [25] showed a clear exponential behavior of $\lambda(T)$ measured using a microwave technique for MgB_2 wires. On the other hand, Pronin *et al.* [26] reported the penetration depth measurements of c -axis oriented films with $T_c \simeq 32$ K. They claimed that the penetration depth shows T^2 temperature dependence rather than exponential behavior at low temperatures, and suggested a strong gap anisotropy or the existence of nodes in the gap as its origin. At present, some of the results of penetration depth measurements and their interpretations are still controversial.

In this work, we measure the magnetic penetration depth of a high-quality MgB_2 film via a mutual-inductance technique. At low temperatures, the superfluid density, $\rho_s \propto \lambda^{-2}(T)$, shows a clear exponential temperature dependence. However, the model assuming a single gap does not describe the experimental results. A full calculation within the BCS framework assuming existence of a double gap, successfully describes our data. The values of the two gaps obtained from fits to the data are consistent with previous reports. Also, the contributions of each gap to the superfluid density are deduced from the analysis.

Initially, we compare the data with the low-temperature expansion formula for $\lambda^{-2}(T)$ assuming one or two gaps to get a rough estimate of the gap values. Then, we refine the values from a full calculation of the penetration depth. Finally, we consider how the penetration depth is affected by gap anisotropy.

II. EXPERIMENTAL ASPECTS

The MgB₂ thin film was fabricated using a two-step method; the detailed process is described elsewhere. [27] First, an amorphous boron thin film was deposited on a (1 $\bar{1}$ 0 2) Al₂O₃ substrate of 1 × 1 cm² at room temperature by pulsed laser. Then, the boron thin film was put into a Nb tube with high purity Mg metal (99.9%), and the Nb tube was then sealed using an arc furnace in an Ar atmosphere. Finally, the heat treatment was carried out at 900°C for 10 to 30 minutes in an evacuated quartz ampoule, which was sealed under high vacuum. The film thickness is 0.3 μm, confirmed by scanning electron microscopy. X-ray diffraction patterns indicated that the MgB₂ thin film has a highly *c*-axis-oriented crystal structure normal to the substrate surface; no impurity phase is observed.

The penetration depth, $\lambda(T)$, was measured using a two-coil mutual inductance technique described in detail elsewhere. [28,29] The MgB₂ film is centered between drive and pick-up coils with diameter of ~ 1 mm. The inset of Fig. 1 schematically illustrates the measurement configuration. A current ($1 \text{ mA} \leq I_d \leq 30 \text{ mA}$) at 50 kHz in the drive coil induces screening currents in the film. The net magnetic field from the drive coil and the induced current in film are measured as a voltage across the pick-up coil. Because the coils are much smaller than the film, the applied field is concentrated near the center of the film and demagnetizing effects at the film perimeter are not relevant. All data presented here are taken in the linear response regime. Figure 1 shows representative mutual inductance, $M(T)$, data measured with $I_d \simeq 30 \text{ mA}$ for $T \leq 25 \text{ K}$ and $I_d \simeq 2 \text{ mA}$ for $T \geq 25 \text{ K}$. The mutual inductance technique enables us to extract absolute values as well as temperature dependence of the penetration depth from the mutual inductance data.

The procedure to extract $\lambda^{-2}(T)$ from $M(T)$ is the following: First, a constant background (zero position) due to stray couplings between coils is subtracted from raw data. This constant background can be estimated from measuring at $T = 4.2 \text{ K}$ the mutual inductance of Pb foil with identical shape and area as substrate using the same measurement probe. In this background measurement, the magnetic penetration depth of Pb is so small compared to foil thickness that no magnetic field goes through film. After the subtraction of the background, the data is normalized to the value of mutual inductance at $T = 50 \text{ K}$ (initial position). The normalization removes uncertainties associated with amplifier gains and nonideal aspects of the coil windings. The subtracted and normalized mutual inductance is converted to complex conductivity, $\sigma = \sigma_1 - i\sigma_2$, where σ_1 and σ_2 are real and imaginary parts of the conductivity. Finally, the penetration depth is determined from the imaginary part of conductivity via the relationship $\sigma_2 = 1/\mu_0\omega\lambda^2$, where μ_0 is the magnetic permeability of vacuum and ω is the frequency of drive current. The accuracy of λ^{-2} is limited by 10% uncertainty in film thickness. However, the temperature dependence of λ^{-2} is unaffected by the uncertainty. The other inset of Fig. 1 displays $\lambda^{-2}(T)$ curves deduced from $M(T)$ measured at two different I_d levels. Although the signal-to-noise ratio of upper curve ($I_d = 10 \text{ mA}$ for $T \leq 25 \text{ K}$) is smaller than that of lower one ($I_d = 30 \text{ mA}$ for $T \leq 25 \text{ K}$), two curves do not show any quantitative difference. (Upper curve was shifted by $10 \mu\text{m}^{-2}$ for comparison.)

III. RESULTS AND DISCUSSION

A. Theoretical description of data assuming a single gap

Figure 2 shows $\lambda^{-2}(T)$ at temperatures below 15 K. The value of $\lambda^{-2}(T)$ at $T \simeq 1.3 \text{ K}$ is about $43 \mu\text{m}^{-2}$, which corresponds to $\lambda \simeq 150 \text{ nm}$. To examine the temperature dependence of $\lambda^{-2}(T)$ at low temperatures, we fit first $\sim 5\%$ drop in $\lambda^{-2}(T)$ to an exponential-type function $\lambda^{-2}(T) \sim 1 - c \exp(-D/T)$, where c and D are adjustable parameters. As presented by thin solid line in the figure, the fit is reasonably good. On the other hand, when we fit the data in the same temperature region to a quadratic form $\lambda^{-2}(T) \sim 1 - (T/T_0)^2$ as in Ref. [22,26], the fit deviates significantly from the data (dashed line in the same figure). The χ^2 values for exponential and quadratic fits are 3.96×10^{-5} and 5.13×10^{-4} , respectively.

The exponential T -dependence of $\lambda^{-2}(T)$ at low temperatures can be regarded to reflect *s*-wave order-parameter symmetry in this compound. For clean BCS-type superconductors [30], $\lambda^{-2}(T)$ is given by

$$\frac{\lambda^{-2}(T)}{\lambda^{-2}(0)} = 1 - 2 \int_{\Delta}^{\infty} \left(-\frac{\partial f(E)}{\partial E} \right) D(E) dE, \quad (1)$$

where Δ is the superconducting energy gap, $f(E) \equiv [\exp(-E/k_B T) + 1]^{-1}$ is the Fermi distribution function, and $D(E) \equiv E/(E^2 - \Delta^2)^{1/2}$, is the quasiparticle density of states (DOS). This equation can be expanded at low temperatures, where Δ is nearly constant, in the following way [31]:

$$\frac{\lambda^{-2}(T)}{\lambda^{-2}(0)} \simeq 1 - \left(\frac{2\pi\Delta(0)}{k_B T} \right)^{1/2} \exp(-\Delta(0)/k_B T), \quad (2)$$

where $\Delta(0)$ is the energy gap at zero temperature. Thin solid line in Fig. 3 represents Eq.(2) fitted to data. The comparison between data and theory is restricted to the first $\sim 5\%$ drop in $\lambda^{-2}(T)$, where the T -dependence of Δ is not significant. This comparison yields $\Delta(0) = 4.29$ meV [$\Delta(0)/k_B T_c = 1.31$] and $\lambda^{-2}(0) = 43.2 \mu\text{m}^{-2}$. The gap value is significantly smaller than the BCS weak coupling limit $\Delta(0)/k_B T_c \simeq 1.76$. Using the gap value deduced above, $\lambda^{-2}(T)$ in the whole temperature region below T_c can be obtained by a full BCS calculation using Eq. (1). If the above one-gap fit is valid, the full calculation is expected to describe the experimental $\lambda^{-2}(T)$ for the entire temperature region below T_c . Thin solid line in the inset of Fig. 3 represents this full calculation. The curve does not give a correct description of the data at high temperatures. While the data show negative curvature at high temperatures, the theoretical line shows weakly positive curvature.

B. Theoretical description of data assuming a double gap

A number of experimental and theoretical groups have proposed the existence of two gaps in the DOS of MgB_2 . The larger gap belongs to the quasi-2D Fermi surface derived from B-B (σ) bonds, and the smaller gap belongs to the quasi-3D Fermi surface derived from B-Mg-B (π) bonds. We model this two-gap nature by writing $D(E)$ as a sum of two BCS DOS. Thus, low-temperature expansion of $\lambda^{-2}(T)$ can be expressed by

$$\lambda^{-2}(T) \simeq \lambda_S^{-2}(0) \left[1 - \left(\frac{2\pi\Delta_S(0)}{k_B T} \right)^{1/2} \exp(-\Delta_S(0)/k_B T) \right] + \lambda_L^{-2}(0) \left[1 - \left(\frac{2\pi\Delta_L(0)}{k_B T} \right)^{1/2} \exp(-\Delta_L(0)/k_B T) \right],$$

where the $\Delta_S(0)$ [$\Delta_L(0)$] and $\lambda_S^{-2}(0)$ [$\lambda_L^{-2}(0)$] are the value of the small (large) gap and the contribution of small (large) gap to total superfluid density ($\propto \lambda^{-2}$), respectively. For comparison with data, it is more convenient to convert the above equation to the following form

$$\frac{\lambda^{-2}(T)}{\lambda^{-2}(0)} \simeq 1 - c_1 \left(\frac{2\pi\Delta_S(0)}{k_B T} \right)^{1/2} \exp(-\Delta_S(0)/k_B T) - c_2 \left(\frac{2\pi\Delta_L(0)}{k_B T} \right)^{1/2} \exp(-\Delta_L(0)/k_B T), \quad (3)$$

where $\lambda^{-2}(0) = \lambda_S^{-2}(0) + \lambda_L^{-2}(0)$, $c_1 = \lambda_S^{-2}(0)/\lambda^{-2}(0)$, and $c_2 = (1 - c_1)$.

At very low temperatures, the change of superfluid density with temperature, i.e., the quasiparticle excitation, is dominated by the small gap. In other words, the role of the large gap in $\lambda^{-2}(T)$ is relevant at higher temperatures. Thus, we extend the fitting region up to $\sim 15\%$ drop in $\lambda^{-2}(T)$. 15% drop in $\lambda^{-2}(T)$ corresponds to about 10% drop in $\Delta(T)/\Delta(0)$ in the BCS weak coupling limit. Accordingly, in this fit about 10% error due to change of Δ can be expected. Figure 4 shows the comparison of Eq. (3) with data. From this fit, we obtain two distinct gap values, $\Delta_S(0) = 2.57$ meV and $\Delta_L(0) = 5.82$ meV, corresponding to $\Delta_S(0)/k_B T_c = 0.79$ and $\Delta_L(0)/k_B T_c = 1.78$. In the case of the small gap, the value is consistent with previous reports. But the large gap value is somewhat smaller than those in the literatures (Table I).

The success of the fit motivates a full calculation in the extended temperature range for a more precise description of the data. We assume isotropic s -wave gaps on the two pieces of Fermi surface, and perform a full calculation of $\lambda^{-2}(T)$ according to

$$\frac{\lambda^{-2}(T)}{\lambda^{-2}(0)} = 1 - 2 \left[c_1 \int_{\Delta_S}^{\infty} \left(-\frac{\partial f}{\partial E} \right) D_S(E) dE + c_2 \int_{\Delta_L}^{\infty} \left(-\frac{\partial f}{\partial E} \right) D_L(E) dE \right], \quad (4)$$

where c_1 is adjustable parameter which determines the contribution of the small gap to the superfluid density and $c_2 = (1 - c_1)$.

Figure 5 shows our attempt to fit the data using Eq.(4). Except near T_c , the theoretical line gives a good fit to the data. From this, we obtain the gap values $\Delta_S(0) = 2.61 \pm 0.41$ meV and $\Delta_L(0) = 6.50 \pm 0.33$ meV. These are fairly consistent with previous reports (Table I). Also, the contributions of each gap to $\lambda^{-2}(0)$, i.e., $c_2 = 0.79 \pm 0.06$ is deduced. The inset of Fig. 5 shows theoretical $\lambda^{-2}(T)$ curves, where the contributions of each gap are separately plotted.

In the above analysis, we described the $\lambda^{-2}(T)$ theoretically assuming the gaps (Δ_L and Δ_S) being isotropic on the Fermi surfaces. According to a recent theoretical calculation, the values of the small and large gaps are distributed in the range of $1 \text{ meV} \leq \Delta_S \leq 3 \text{ meV}$ and $6.5 \text{ meV} \leq \Delta_L \leq 7.5$ on the Fermi surfaces. [6] Here we suppose two phenomenological models for gap distribution. In the first model, the gap is distributed uniformly around the average value of gap, Δ_0 . In the alternative model, we assume the normal (Gaussian) distribution of the gap. Using these models, we calculate theoretical curves of $\lambda^{-2}(T)$ assuming $\sim \pm 25\%$ variation of gap around Δ_0 on the Fermi surface. The gap distribution of $\pm 25\%$ is sufficient to account for real gap anisotropy in MgB_2 . [13] The calculations reveal that the change in $\lambda^{-2}(T)$ due to the gap distribution is not significant. In fact, the maximum change in λ^{-2} due to the gap anisotropy is only about 2% in the case of the uniform distribution. The normal gap distribution causes negligibly small change in λ^{-2} . These results lead us to the conclusion that the gap anisotropy on the Fermi surface of MgB_2 is not relevant in determining the temperature dependence of the penetration depth.

IV. SUMMARY

The magnetic penetration depth $\lambda(T)$ of a high-quality, *c*-axis oriented MgB_2 film was obtained from mutual-inductance measurements in the linear-response regime. The exponential temperature dependence of $\lambda^{-2}(T)$ at low temperatures suggests a nodeless gap on the Fermi surface. However, the data could not be described by the *s*-wave theory assuming a single gap even at low temperatures. On the other hand, the data were successfully described by the full calculation of $\lambda^{-2}(T)$ with two distinct gap values: $\Delta_S(0) = 2.61 \pm 0.41 \text{ meV}$ and $\Delta_L(0) = 6.50 \pm 0.33 \text{ meV}$. At $T = 0$, the contribution of the small gap to the superfluid density was found to be 21%. Finally, two phenomenological models to account for gap-size distribution on the Fermi surface were considered. It was found that gap-size distribution in MgB_2 does not play a significant role in determining the temperature dependence of the penetration depth.

ACKNOWLEDGMENTS

This work was supported in part by DOE Grant DE-FG02-90ER45427 through the Midwest Superconductivity Consortium (MSK, JAS, and, TRL) and by Creative Research Initiatives of the Korean Ministry of Science and Technology (WNK, HJK, EMC, and SIL).

TABLE I. Summary of previously reported superconducting gap values of MgB_2 superconductor.

Δ_S (Δ), meV	Δ_L , meV	Tool	Refs.
2.61 ± 0.41	6.5 ± 0.33	Penetration depth	this work
$1 \sim 3$	$6.5 \sim 7.5$	First principle calc.	Ref.[5]
2.5	-	Tunneling	Ref.[8]
3.8	7.8	STM	Ref.[9]
1.7	7	Point-contact spec.	Ref.[10]
2.8	7	Point-contact spec.	Ref.[11]
2.45 ± 0.15	7.0 ± 0.45	Point-contact spec.	Ref.[13]
1.7	5.6	Photoemission spec.	Ref.[19]
2.7	6.2	Raman spec.	Ref.[20]
2.8 ± 0.4	-	Penetration depth	Ref.[23]
2.61	-	Penetration depth	Ref.[25]

-
- [1] J. Nagamatsu, N. Nakagawa, T. Muranaka, Y. Zenitani, and J. Akimitsu, *Nature* **410**, 63 (2001).
 - [2] S. L. Bud'ko, G. Lapertot, C. Petrovic, C. E. Cunningham, N. Anderson, and P. C. Canfield, *Phys. Rev. Lett.* **86**, 1877 (2001).
 - [3] W. L. McMillan and J. M. Rowell, in *Superconductivity*, edited by R. D. Parks (Marcel Dekker, New York, 1969), p. 561.
 - [4] A. Y. Liu, I. I. Mazin, and J. Kortus, *Phys. Rev. Lett.* **87**, 087005 (2001).
 - [5] H. J. Choi, D. Roundy, H. Sun, M. L. Cohen, and S. G. Louie, *cond-mat/0111183*, 2001.
 - [6] H. J. Choi, D. Roundy, H. Sun, M. L. Cohen, and S. G. Louie, *cond-mat/0111182*, 2001.
 - [7] A. A. Golubov, J. Kortus, O. V. Dolgov, O. Jepsen, Y. Kong, O. K. Andersen, B. J. Gibson, K. Ahn, and R. K. Kremer, *cond-mat/0111262*, 2001.
 - [8] H. Schmidt, J. F. Zasadzinski, K. E. Gray, and D. G. Hinks, *Phys. Rev. B* **63**, 220504 (2001).
 - [9] F. Giubileo, D. Roditchev, W. Sacks, R. Lamy, D. X. Thanh, J. Klein, S. Miraglia, D. Fruchart, J. Marcus, and Ph. Monod, *Phys. Rev. Lett.* **87**, 177008 (2001).
 - [10] F. Laube, G. Goll, J. Hagel, H. v. Lohneysen, D. Ernst, and T. Wolf, *cond-mat/0106407*, 2001.
 - [11] P. Szabó, P. Samuely, J. Kačmarčík, T. Klein, J. Marcus, D. Fruchart, S. Miraglia, C. Marcenat, and A. G. M. Jansen, *Phys. Rev. Lett.* **87**, 137005 (2001).
 - [12] P. Seneor, C.-T. Chen, N.-C. Yeh, R. P. Vasquez, L. D. Bell, C. U. Jung, Min-Seok Park, Heon-Jung Kim, W. N. Kang, and Sung-Ik Lee, *Phys. Rev. B* **65**, 012505 (2001).
 - [13] Yu. G. Naidyuk, I. K. Yanson, L. V. Tyutrina, N. L. Bobrov, P. N. Chubov, W. N. Kang, H.-J. Kim, E.-M. Choi, and S.-I. Lee, *cond-mat/0112452*, 2002.
 - [14] F. Bouquet, R. A. Fisher, N. E. Phillips, D. G. Hinks, and J. D. Jorgensen, *Phys. Rev. Lett.* **87**, 047001 (2001).
 - [15] Y. Wang, T. Plackowski, and A. Junod, *Physica C* **355**, 179 (2001).
 - [16] H. D. Yang, J.-Y. Lin, H. H. Li, F. H. Hsu, C. J. Liu, S.-C. Li, R.-C. Yu, and C.-Q. Jin, *Phys. Rev. Lett.* **87**, 167003 (2001).
 - [17] Ch. Wälti, E. Felder, C. Degen, G. Wigger, R. Monnier, B. Delley, and H. R. Ott, *Phys. Rev. B* **64**, 172515 (2001).
 - [18] H. Kotegawa, K. Ishida, Y. Kitaoka, T. Muranaka, and J. Akimitsu, *Phys. Rev. Lett.* **87**, 127001 (2001).
 - [19] S. Tsuda, T. Yokoya, T. Kiss, Y. Takano, K. Togano, H. Kito, H. Ihara, and S. Shin, *Phys. Rev. Lett.* **87**, 177006 (2001).
 - [20] X. K. Chen, M. J. Konstantinovic, J. C. Irwin, D. D. Lawrie, and J. P. Franck, *Phys. Rev. Lett.* **87**, 157002 (2001).
 - [21] J. Kortus, I. I. Mazin, K. D. Belashchenko, V. P. Antropov, and L. L. Boyer, *Phys. Rev. Lett.* **86**, 4656 (2001).
 - [22] C. Panagopoulos, B. D. Rainford, T. Xiang, C. A. Scott, M. Kambara, and I. H. Inoue, *Phys. Rev. B* **64**, 094514 (2001).
 - [23] F. Manzano, A. Carrington, N. E. Hussey, S. Lee, A. Yamamoto, and S. Tajima, *Phys. Rev. Lett.* **88**, 047002 (2002).
 - [24] G. Lamura, E. Di Gennaro, M. Salluzzo, A. Andreone, J. Le Coche, A. Gauzzi, C. Cantoni, M. Paranthaman, D. K. Christen, H. M. Christen, G. Giunchi, and S. Ceresara, *Phys. Rev. B* **65**, 020506 (2002).
 - [25] R. Prozorov, R. W. Giannetta, S. L. Bud'ko, and P. C. Canfield, *Phys. Rev. B* **64**, 180501 (2001).
 - [26] A. V. Pronin, A. Pimenov, A. Loidl, and S. I. Krasnovobodtsev, *Phys. Rev. Lett.* **87**, 097003 (2001).
 - [27] W. N. Kang, H.-J. Kim, E.-M. Choi, C. U. Jung, and S.-I. Lee, *Science* **292**, 1521 (2001).
 - [28] S. J. Turneaure, E. R. Ulm, and T. R. Lemberger, *J. Appl. Phys.* **79**, 4221 (1996).
 - [29] S. J. Turneaure, A. A. Pesetski, and T. R. Lemberger, *J. Appl. Phys.* **83**, 4334 (1998).
 - [30] M. Tinkham, *Introduction to Superconductivity*, 2nd ed. (McGraw-Hill, New York, 1996).
 - [31] J. Halbritter, *Z. Physik* **243**, 201 (1971).

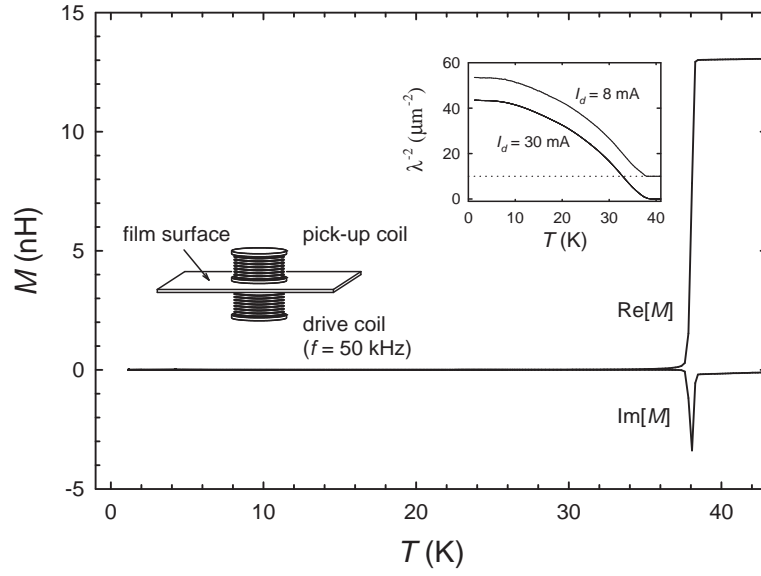


FIG. 1. Representative complex mutual inductance $M(T)$ of MgB_2 measured using two-coil method. Inset (left) shows schematic diagram of measurement configuration. Inset (right) shows $\lambda^{-2}(T)$ curves extracted from $M(T)$ measured at different current levels. Upper cu

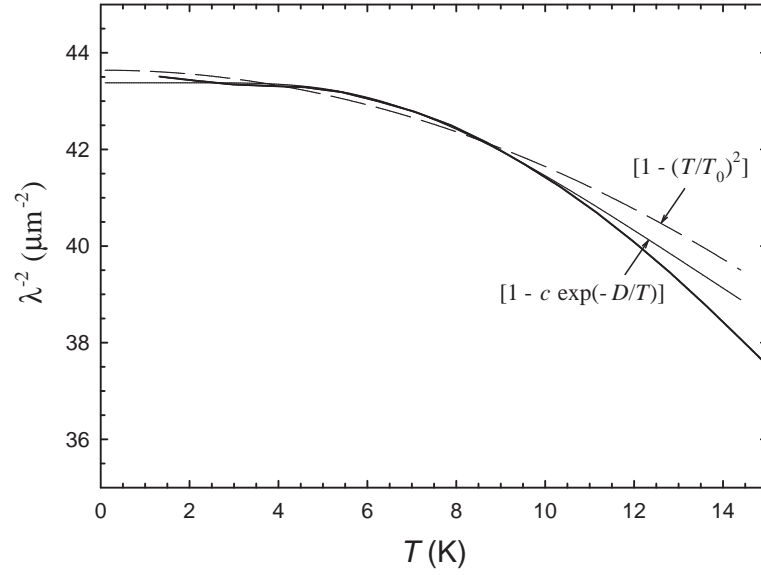


FIG. 2. $\lambda^{-2}(T)$ of MgB_2 film at low temperatures. Thin solid and dashed lines denote best fits of $\lambda^{-2}(0)[1 - c \exp(-D/T)]$ and $\lambda^{-2}(0)[1 - (T/T_0)^2]$ to the data, respectively.

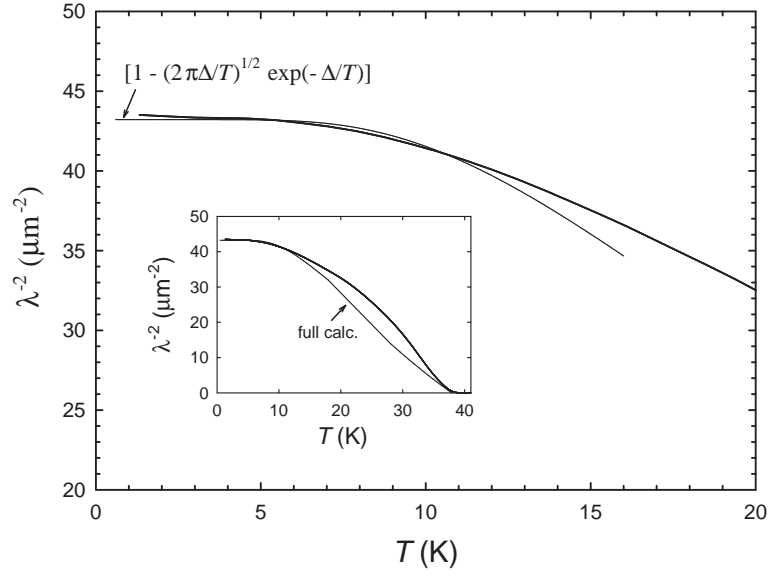


FIG. 3. $\lambda^{-2}(T)$ of MgB_2 film at low temperatures. Thin solid line denotes a best fit of Eq.(2). From this fit, $\Delta(0) = 4.29$ meV ($\Delta(0)/k_B T_c = 1.31$) was obtained. Inset: $\lambda^{-2}(T)$ for temperatures below T_c . Thin solid line is a full BCS calculation assuming $\Delta(0) = 4.29$ meV.

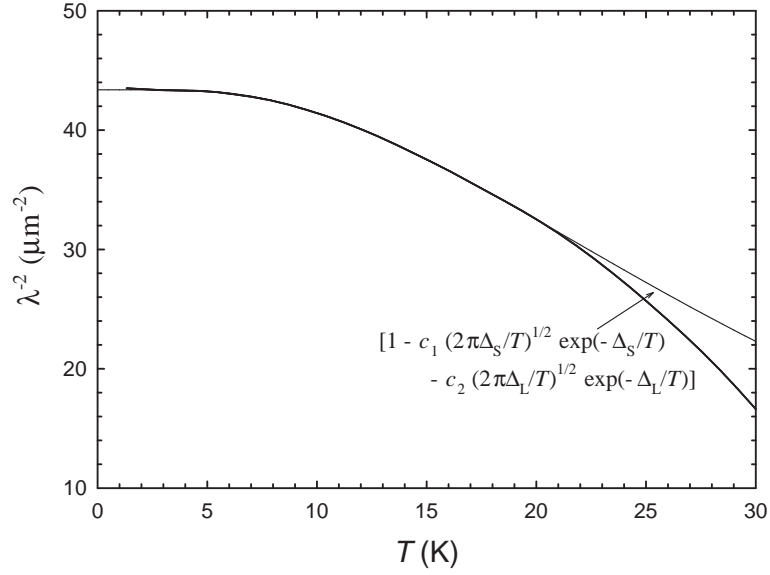


FIG. 4. $\lambda^{-2}(T)$ fitted by Eq.(3). In this fit, the values of two distinct gaps $\Delta_S(0) = 2.57$ meV and $\Delta_L(0) = 5.82$ meV were obtained.

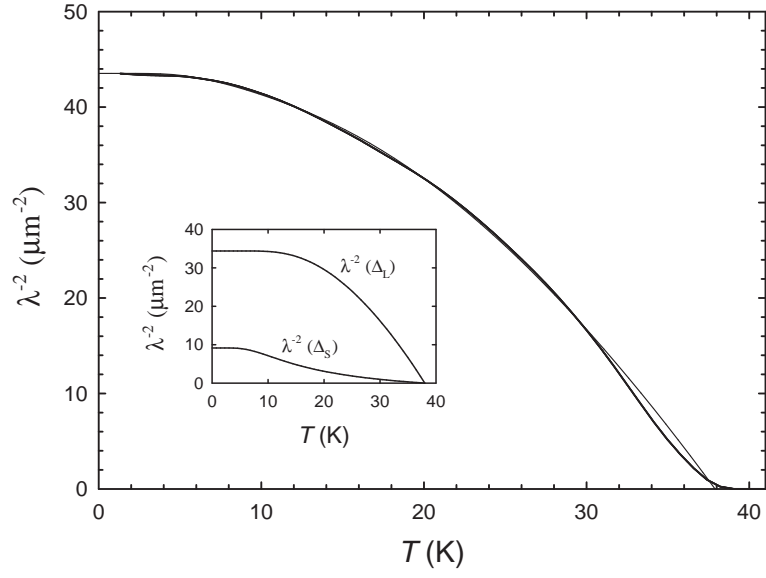


FIG. 5. $\lambda^{-2}(T)$ for whole temperature range below T_c . Thin solid line is a full BCS calculation of $\lambda^{-2}(T)$ assuming two distinct gaps. From this, refined gaps values $\Delta_S(0) = 2.61$ meV and $\Delta_L(0) = 6.50$ meV were obtained. Inset: Theoretical curves of $\lambda^{-2}(T)$. Upper and lower curves are the contributions of the large ($\Delta_L(0) = 6.50$ meV) and the small ($\Delta_S(0) = 2.61$ meV) gaps, respectively.